

**Embedded
Code Generation**
DEMO MODEL

DC Microgrid

Microgrid with two battery storage systems, a grid interface converter, a constant power load and PV production

Last updated in C2000 TSP 1.6.1

www.plexim.com

- ▶ Request a PLECS and PLECS Coder trial license
- ▶ Get the latest TI C2000 and RT Box Target Support Package
- ▶ Check the PLECS, RT Box and TI C2000 TSP documentation

1 Overview

This demo model shows the simulation of a bipolar low-voltage DC microgrid. The microgrid is composed of the following main elements:

- **Two Battery Storage Systems (BSS):** Each of the two battery storage systems consists of two dual active bridges with their inputs in series and outputs in parallel. Both BSSs are controlling the bipolar DC power link voltage. Each BSS delivers a rated power of 20 kW and a switching frequency of 15 kHz. Every BSS will act as a grid-supporting converter on the microgrid. Which means that they are not only able to maintain the DC-bus voltage stable, but also to control the power flow among the two paralleled converters. To achieve this parallel operation of both BSSs, droop control is applied.
- **Grid Interface Converter (GIC):** An NPC (neutral point clamped) voltage source inverter is used as the interface between the common DC power link and the low-voltage utility AC grid. The nominal power of the inverter is 20 kW. The switching frequency was selected as 20 kHz. Since the grid interface converter is power controlled, it acts as a constant power load on the common DC power link.
- **Constant power loads (CPL):** A simplified model of a constant power load is implemented by means of a voltage controlled current source with limited bandwidth. The power drawn by the load is variable and can be changed during the simulation.
- **PV production:** PV production is emulated by a controlled current source. The installed peak power can be adjusted freely during simulation.

This document provides an explanation of the typical workflow of the PLECS Embedded Coder using Texas Instruments (TI) C2000 MCUs. Combined with a PLECS RT Box, the performance of the MCU can be verified directly. The entire DC microgrid model runs on a total of 4 RT Boxes.

Note This model contains model initialization commands that are accessible from:

PLECS Standalone: The menu **Simulation + Simulation Parameters... + Initializations**

PLECS Blockset: Right click in the **Simulink model window + Model Properties + Callbacks + InitFcn***

2 Model

A microgrid is a local electrical energy grid that interconnects loads, storage and generation within a clearly defined electrical boundary and that acts as a single controllable entity with respect to the mains utility AC grid. Such a microgrid can either operate under grid-connected or islanded mode. Under grid-connected operation the microgrid can exchange energy in a controlled way with the mains AC grid. In islanded mode the microgrid is disconnected from the utility grid and has to feed all loads independently. The common power feeder of a microgrid can either be AC or DC. In this demo model there is a DC common power feeder and the microgrid can operate in grid-connected and islanded mode. The voltage level of the common DC-bus is ± 375 V.

The model is composed of different subsystems. Hereafter a short overview is given for each subsystem:

- **DC Power Grid:** This subsystem includes the passive structure of the DC microgrid. The different power electronics converters are interconnected by a parasitic line impedance. Additionally, PV production and a constant power load (CPL) are emulated in this subsystem.
- **BSS1 plant:** This subsystem includes the power circuit of the first battery storage system. Each BSS consists of two dual active bridges with their input sides in series and the output sides connected in parallel. The same is true for the subsystem “BSS2 plant”.
- **BSS1 controller:** This subsystem includes the control loops for the battery storage system 1. To enable load sharing, a local droop controller is implemented. The subsystem “BSS2 controller” is implemented in the same way.

- GIC plant: This subsystem includes the power circuit of the grid interlinking converter. This converter interfaces the DC microgrid with the three-phase AC grid.
- GIC controller: The “GIC controller” subsystem includes the control loop for the AC/DC inverter.

The following sections discuss each subsystem in depth. Optionally, skip to section 3 to view instructions on running the real-time simulation.

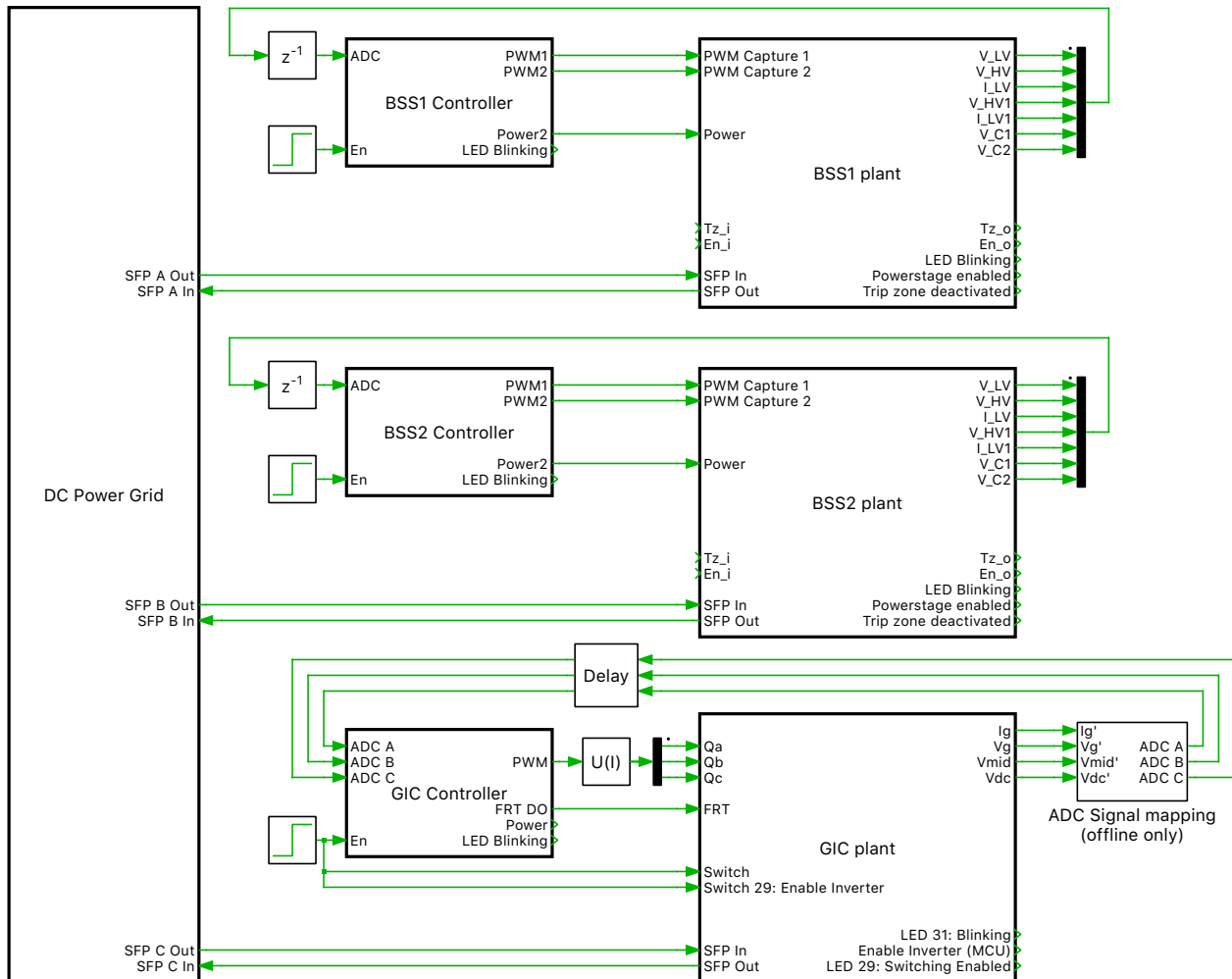


Figure 1: System overview with the 4 subsystems implementing the plants “DC Power Grid”, “BSS1”, “BSS2” and “GIC” and their respective local controllers.

2.1 DC Power Grid

The passive structure of the DC microgrid runs on a separate RT Box. Each independent converter is connected through a line impedance to the common DC power link. The CPL and PV system represent the dynamic load and generation profiles of the microgrid. For offline simulation the time vector is compressed into 1 second. The variable `DCgrid.plant.time_scaling` can be used to change the scaling of the time vector.

PV Production

In the masked subsystem “PV Production” a simplified model of a PV power plant is implemented, as shown in Fig. 3. The peak power level can be adjusted in the initialization commands by modifying the

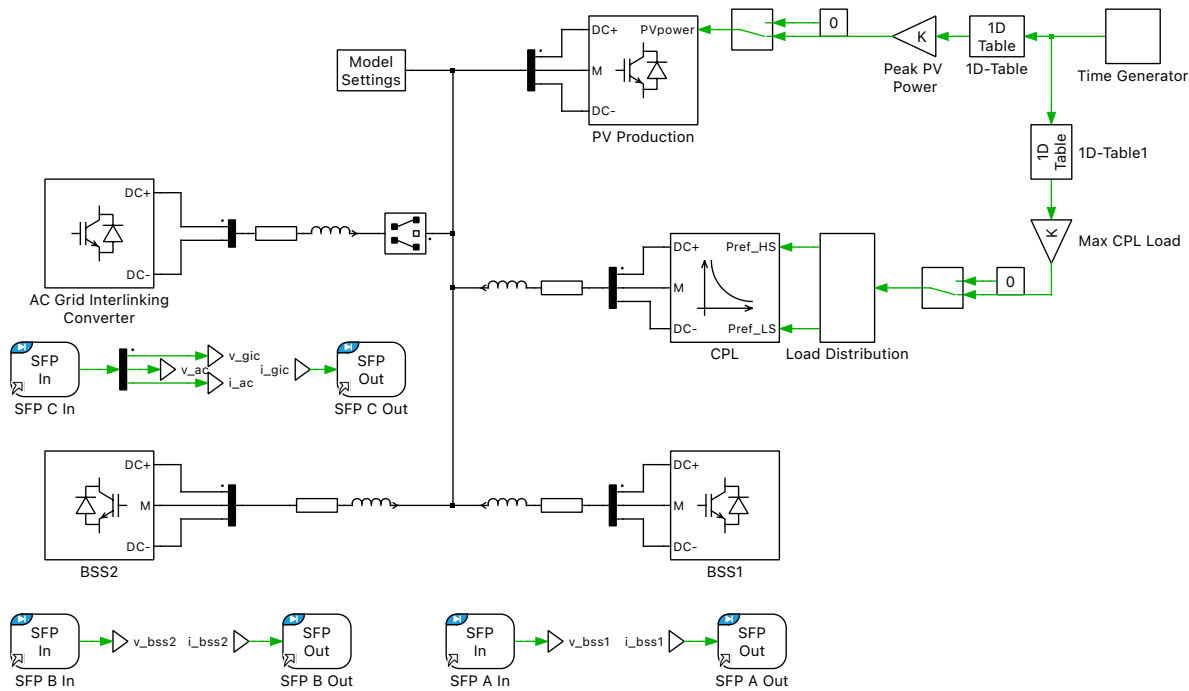


Figure 2: Schematic of the DC grid

variable `DCgrid.plant.PVpeak_power`. The initial value of the peak power is set to 10 kW. The control signal for the controlled current source is calculated by dividing the demanded power by the measured DC-bus voltage. To avoid the occurrence of an algebraic loop, first-order low-pass filters limits the dynamic of the current. If the DC-bus voltage is below 650 V, the current source is always set to 0 A.

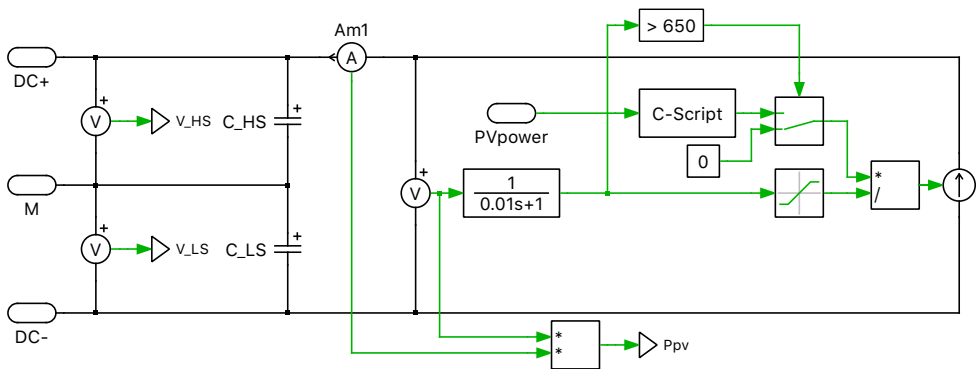


Figure 3: Implementation of the PV production

Constant Power Load

Fig. 4 shows the implementation of the constant power load. The CPL can load the bipolar DC-bus unevenly. The constant power load is emulated by a controlled current source. The applied current signal is calculated according the following relationship:

$$I_{CPL} = \frac{P_{ref}}{V_{dc}} \frac{1}{\frac{1}{\omega_c} s + 1}$$

The first-order low-pass filter represents the bandwidth of the current loop controller of the emulated power electronics converter. The cut-off frequency ω_c can be adjusted in the mask dialog of the CPL subsystem.

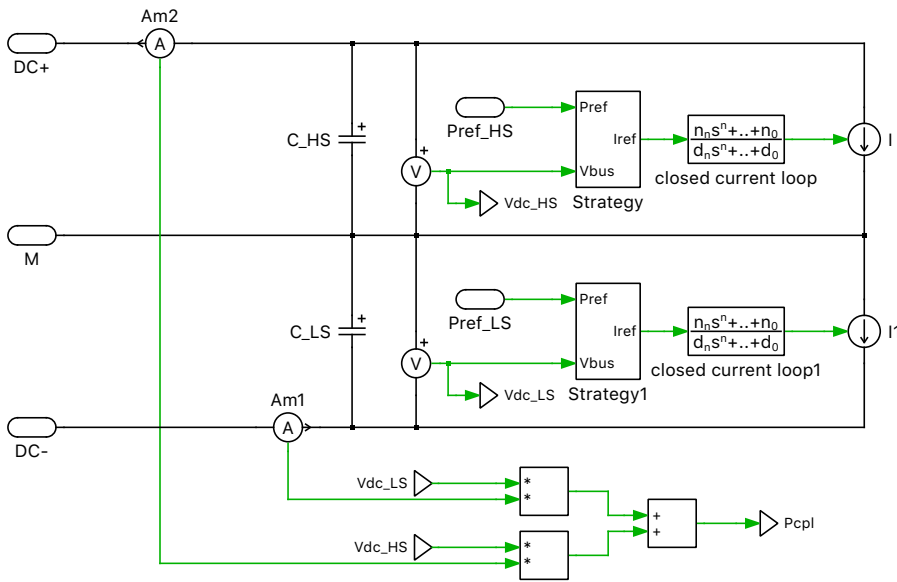


Figure 4: Implementation of the constant power load

2.2 BSS1 and BSS2 plant

Two battery storage systems are connected to the common DC power link. Each power circuit includes a DC-DC converter based on an Input-Series/Output-Parallel Dual Active Bridge (DAB) structure. The input-side (series connection) is connected to the common DC power link, the output-side (parallel connection) interfaces with an electrochemical battery. In order to smooth the power delivered to the battery, an additional filter stage is connected in-between the battery and DAB output. The implementation of the BSS subsystems is given in Fig. 5.

2.3 BSS1 and BSS2 Controllers

The subsystem “BSS Controller” contains the control algorithms for the two BSSs.

Target Blocks

The implementation contains ADC and PWM blocks from the TI C2000 target component library. The measurement of the bipolar DC-link voltages, battery-side voltage and the individual battery-side currents are introduced to the model environment using the ADC blocks from the TI C2000 component library. In order to convert the detected analog voltage into values with physical units to be used by the control algorithm, a scaling factor and an offset are provided for each channel via the parameter window of the ADC block. The ADC unit and the analog input channel parameters can be modified accordingly per available resources of different MCUs.

Droop Control

The two battery storage systems are paralleled and both control the DC-bus voltage. Paralleling converters offers advantages compared to one single high-power converter, such as increased reliability, maintenance under operation and reduced stress on power components. The main challenge of paralleled converters is to achieve load current sharing between the converters and to eliminate current sharing mismatch. To achieve accurate load sharing among the paralleled converters, special control techniques have to be implemented. One simple method is introducing a virtual series resistance in the control loop, i.e. droop-control.

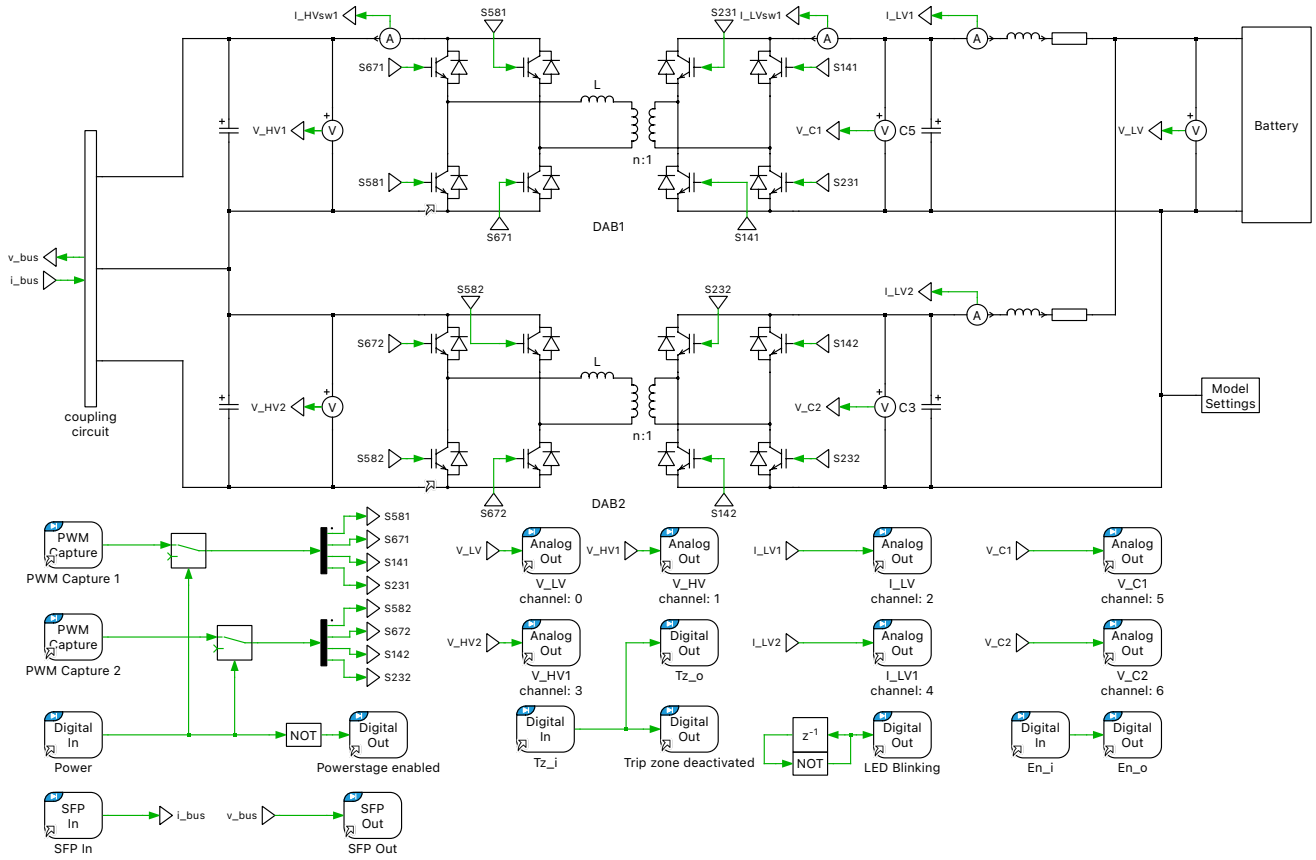


Figure 5: The implementation of the BSS subsystems

The droop controller compares the voltage reference against the measured voltage on the output capacitor. The difference is amplified by a gain, the so-called droop-gain. Selecting an appropriate droop-gain K_{droop} is always a compromise between current sharing accuracy and allowed voltage deviation, as shown in [1]. The higher the droop gain, the smaller the voltage deviation. The smaller the droop gain, the higher the current sharing accuracy.

$$I_{\text{BSS}}^* = K_{\text{droop}}(V^* - V_{\text{meas}})$$

Cascaded Current and Voltage Control

The calculated reference current I_{BSS}^* is an input to the current loop. This outer current loop regulates the current in the filter inductor and provides a voltage reference for the inner voltage controller. Finally, this inner voltage controller provides a current reference which is used to calculate the required phase-shift φ between the primary and secondary full-bridge.

To achieve a controlled ramping of the DC-bus voltage during startup-up, a simple finite state machine is implemented. If the total DC-bus voltage is below 750 V at the start-up process, the droop controller is bypassed and a constant current reference of 5 A is applied to the outer current loop to build up the DC voltage. Feeding a constant current into a capacitor leads to ramp up of the voltage on a capacitor.

2.4 GIC plant

The twelve PWM switching signals are sensed by three PWM Capture blocks from the RT Box target support library. The measurements of the DC voltages, AC currents and AC voltages interface with the connected controllers via Analog Out ports. A Digital Out block labeled “Enable Inverter (MCU)” forwards the external digital input signal to a digital output pin of the RT Box. This pin is connected to a

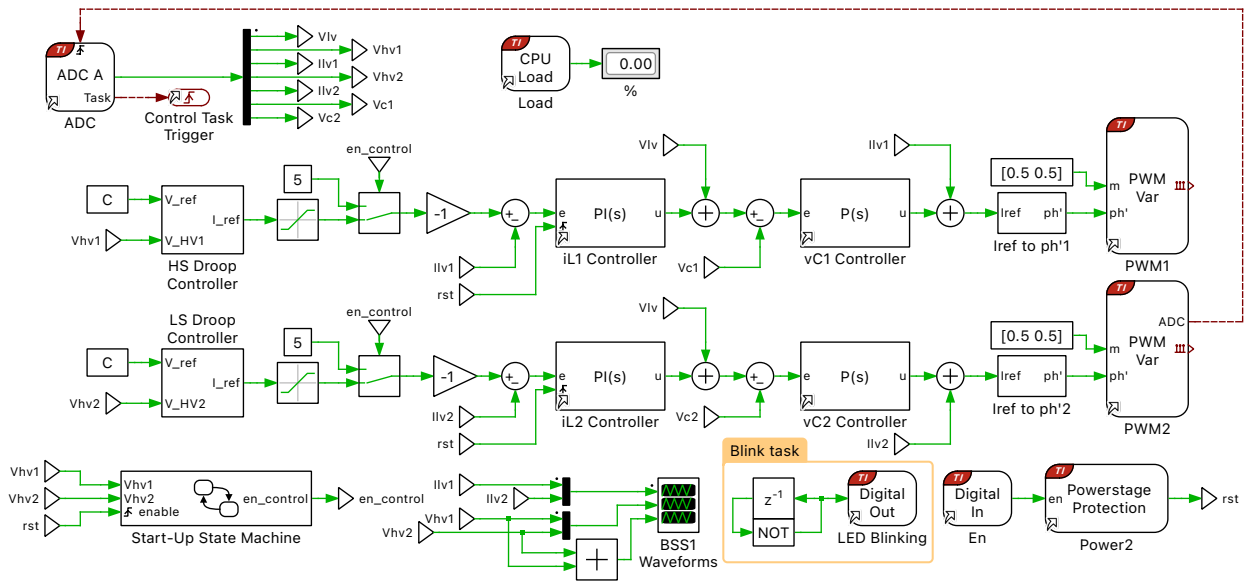


Figure 6: Controller implementation of the two BSSs

GPIO of the MCU to enable/disable PWM outputs via a finite state machine implemented in control software. The mechanism of the MCU's PWM enable/disable function will be elaborated in Section 3.

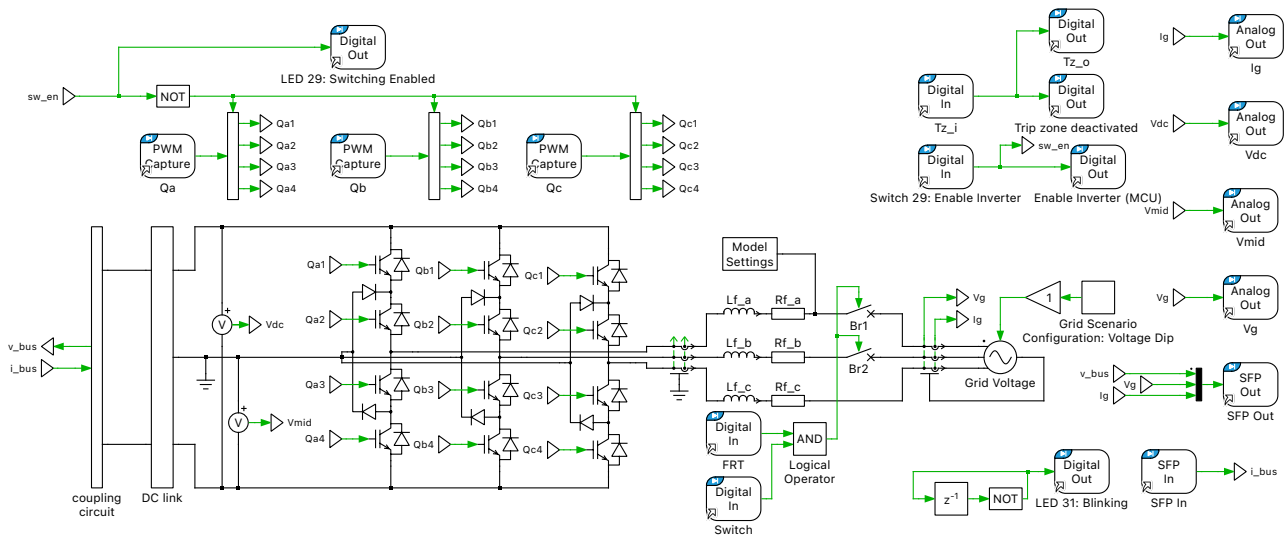


Figure 7: Implementation of the GIC subsystem

2.5 GIC controller

In this subsystem, closed-loop current and power controllers are implemented in a dq frame rotating with angular speed ω , where $\omega = 2\pi f$ and f is the grid frequency. The scheme of the classical control in a rotating frame is shown in Fig. 8. The measurement of the DC-link voltages, AC currents and AC voltages are introduced to the model environment using the ADC blocks from the TI C2000 component library. Active power is controlled in closed-loop. This allows the dynamics of active power to be decided as a consequence of a variation of the grid voltage change. The actual power is calculated based on measurements at the PCC (Point of Common Coupling) and then compared to the respective set-point. A PI-based controller calculates the d component of the reference current.

The i_d and i_q current controllers are designed on the basis of the following plant transfer function:

Both current controllers could be designed based on the same time constant $T = L/R$. The time constant T_1 of the PI-controller is chosen to compensate the time constant of the plant, T . To achieve an optimally damped system (i.e. with 5% overshoot) leads to

where T_s is the switching period.

The phase-locked loop (PLL) of the GIC delivers the actual phase-angle of the AC grid voltage. Additionally, a simple algorithm decides whether the PLL is locked to the grid voltage or not. When the PLL is locked, the boolean signal “SysEnable” is high. Also the grid voltage magnitude is evaluated in the PLL subsystem. A time against voltage characteristic is implemented in the subsystem “FRT”, denoting the minimum requirement for the inverter to stay connected during a voltage dip on the AC grid side. If the grid voltage magnitude during a voltage dip stays above the undervoltage threshold described in Fig. 9 the GIC should remain in operation. If the voltage magnitude is below the threshold, the GIC is disconnected after a clearing time from the AC grid and switching is disabled. Therefore, to enable the switching of the GIC the PLL has to be locked and the AC grid voltage in a normal condition. In addition a global enable has to be given to the controller with a dip-switch connected to an digital input of the MCU.

The entire DC microgrid model runs on a total of 4 RT Boxes. Therefore, the model has to be divided into smaller portions to optimize the execution time on the individual RT Boxes. The circuit is divided by using a coupling circuit as shown in Fig. 10. This model partitioning has to be done at strategic points of the circuit in order to not reduce the stability margins of the model, e.g. next to a capacitor

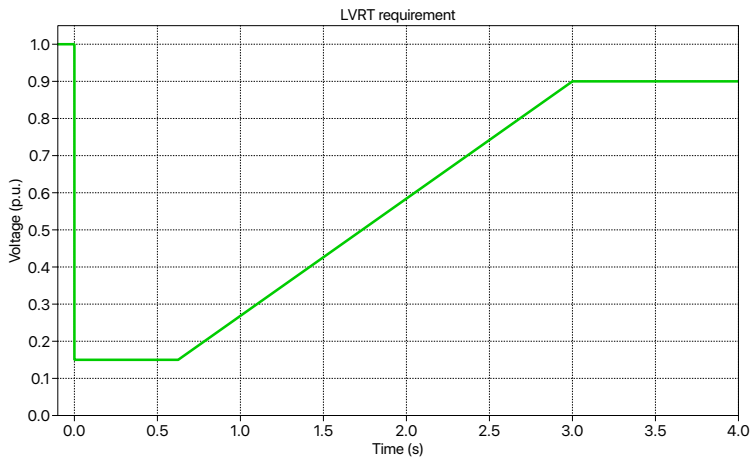


Figure 9: The low voltage ride through requirement, above the limit the generation unit has to stay connected, below the limit it may disconnect from the AC grid.

where the voltage rate of change is limited or next to an inductor where the same is true for the current. As one can see in Fig. 10, the measured current on “Box A” is transferred over SFP to “Box B” and delivers the control signal for the two controlled current sources. The same process can be observed with the measured voltage signals on “Box B”. This coupling circuit, which can be seen as an ideal gyrator with unity gain, enables to split the complex DC microgrid model into smaller pieces, which can be simulated on individual RT Boxes. The left part of the coupling circuit is implemented on one RT Box, the right

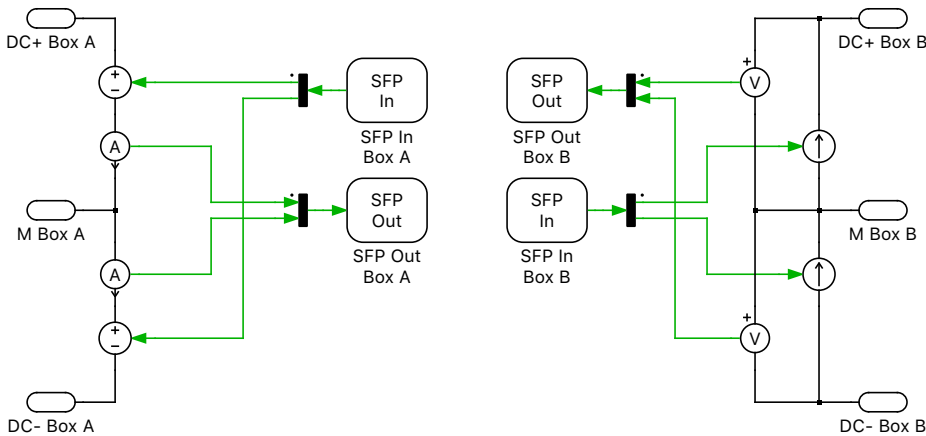


Figure 10: Coupling circuit used to split a circuit among different RT Boxes.

part on a second one. Each converter is connected to the central “DC Power Grid” model by using such a coupling circuit.

3 Simulation

In addition to running a simulation of this demo model in offline mode on a computer, each of the sub-systems can be deployed on a real target by using the PLECS Coder. The CPL and PV system represent the dynamic load and generation profiles of the microgrid. Two BSSs coordinate to regulate the DC link voltage as it changes in response to the net power balance of the load and generation. The GIC supplies a constant 5kW into the AC grid unless a grid fault is detected. If an AC line fault is detected, the GIC controller electrically isolates the DC Microgrid from the AC system, until the fault conditions have elapsed.

Due to the complexity of the model, it has to be split onto 4 PLECS RT Boxes for the HIL verification. Each “plant” subsystem is running on a different RT Box. The RT Box running the “DC Power Grid” subsystems acts as the master for startup. All other RT Boxes act as a slave and synchronize their startup on SFP port A. A schematic overview of the hardware setup is shown in Fig. 11.

3.1 Hardware Setup

The following material is needed to setup a HIL simulation of the DC microgrid model:

- 4x PLECS RT Box 1
- 3x SFP cables
- 3x RT Box LaunchPad Interface
- 2x TI 28069M LaunchPad (for the two BSS controllers)
- 1x TI 28379D LaunchPad (for the GIC controller)

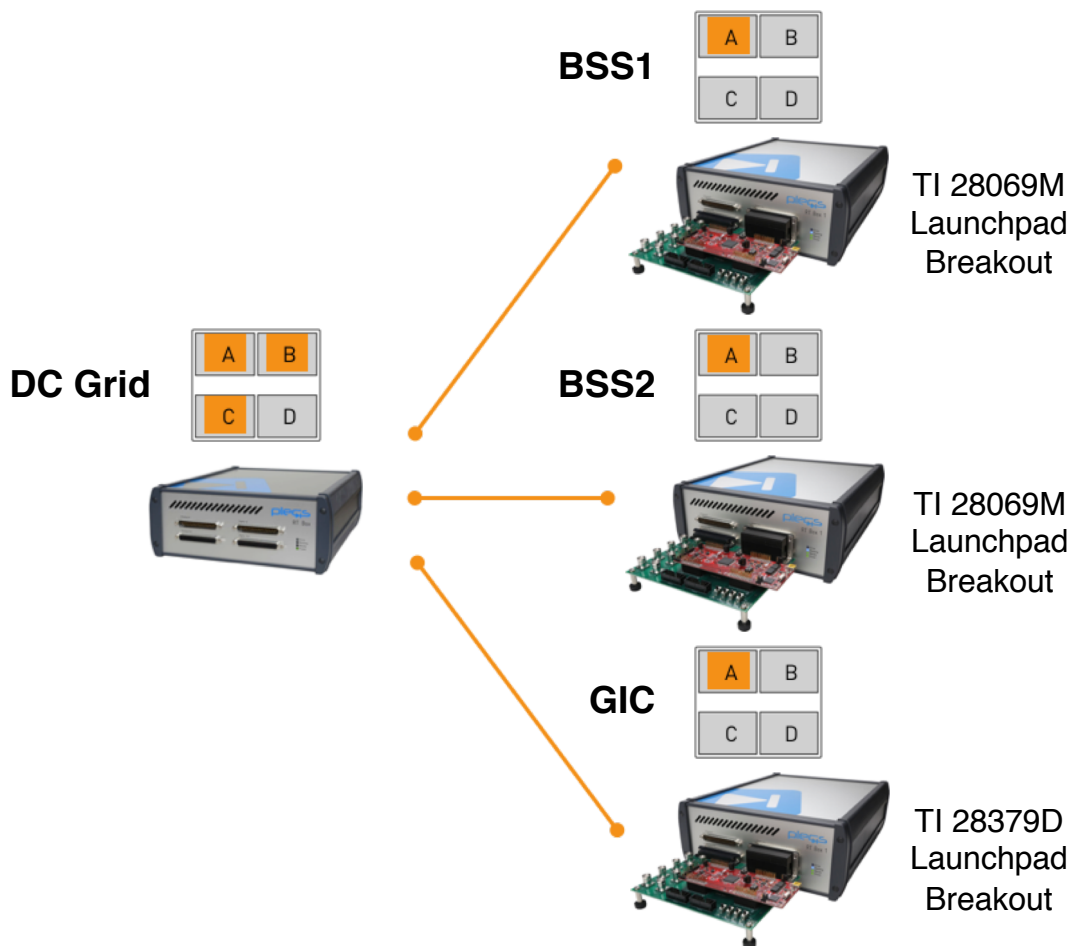


Figure 11: Hardware setup of the HIL verification

To set up the HIL simulation you have to execute the following steps.

- 1** Stack 4 PLECS RT Boxes vertically, labeled as “DC Power Grid”, “BSS1 plant”, “BSS2 plant” and “GIC plant”.
- 2** Connect the SFP cable from the **A**, **B** and **C** ports of the “DC Power Grid” box to the **A** port of the other three boxes, respectively.

- 3 Connect the three RT Box LaunchPad Interface boards to the boxes named “BSS1 plant”, “BSS2 plant” and “GIC plant”. Change the position of all switches in the three interface boards to the position away from the RT Boxes.
- 4 Plug the corresponding LaunchPad to each interface board (TI 28069M LaunchPad [2] for “BSS1 plant” and “BSS2 plant”, TI 28379D LaunchPad [3] for “GIC plant”)
- 5 Download the four plant subsystems to the RT Boxes and the three controller subsystems to the LaunchPads (in arbitrary order).
- 6 After system start (blue LED of all four boxes continuously on), change the position of the “DI28” and “DI29” switch of the interface board of the “BSS1 plant” and/or “BSS2 plant” RT Box pointing towards the RT Box. One of the two (or both) BSS will now start to build up the voltage of the DC-bus.
- 7 Change the “DI28” and “DI29” switch of the “GIC plant” interface board in the position pointing to the RT Box.
- 8 Now, the DC microgrid is running on the four RT Boxes. The three converters are controlled by the three LaunchPads plugged on the interface boards.

Four RT Boxes are stacked to emulate the DC microgrid system that includes a grid interlinking converter, two battery storage systems, a PV production and a constant power load. Different scenarios can be simulated in this microgrid setup:

- AC grid fault scenarios: The GIC is connected to special implementation of a three-phase voltage source. This voltage source enables testing the controller response to abnormal grid conditions, e.g. voltage disturbances, frequency disturbances and changes in the phase-angles. In this demo only undervoltage events are considered. If you set the Gain block to a value between 0 and 1, the GIC will ride through the fault according to the clearing time depicted in Fig. 9.
- Switch off one BSS: During normal operation, the DC-bus voltage is maintained by two BSSs working in parallel. However, a fault in one BSS can be simulated. This can be done by changing the “DI29” switch of one of the two BSS LaunchPad interface boards in the direction away from the RT Box. By doing this, one BSS will stop its operation and the remaining BSS has to take over the whole power needed to balance the DC microgrid.
- The dynamic of the PV production and the CPL can be changed prior to a simulation by changing the variable `DCgrid.plant.time_scaling` in the **Initialization commands** of the model.

The transient results of the simulation can be observed and evaluated using the PLECS Scopes when the **External Mode** is connected.

3.2 Results

The main offline simulation results are shown in Fig. 12. The DC-bus voltage is build up from zero at simulation start. For this, both battery storage systems feed a constant current into the DC-bus. Once the DC-bus voltage reaches 750 V, the controller is switched into droop control and both BSSs control the bus voltage towards 750 V. At around $t = 0.2$ s, the grid interface converter starts to inject a constant power of 5 kW into the AC grid. Also the PV production and the constant power load feed or load the common DC-bus with a variable power level. To achieve voltage control on the DC-bus the two BSSs have to balance the power on the DC power link. This can be summarized as the difference between the total power generation and the total load on the DC-bus:

$$P_{BSS} = P_{PV} - P_{CPL} - P_{GIC}$$

Since both BSSs work in parallel, the power P_{BSS} is distributed on both converters. Even though the droop gain is the same for both BSSs, there is a difference in the power level of the two individual BSS. This can also be observed in Fig. 12. This mismatch is due to the uneven values of the resistive part of the coupling impedance between the converters and the DC-bus.

At $t = 0.5$ s, the AC grid voltage sags down to 0 p.u. Due to this, the GIC-controller stops immediately the switching operation of the AC/DC inverter. Also the circuit breaker between inverter and AC grid is opened. At $t = 0.8$ s, the AC grid voltage is restored back to 1 p.u. This triggers the reconnection of the

inverter. Once the PLL is re-locked to the grid voltage, the GIC starts again to inject the power into the AC grid.

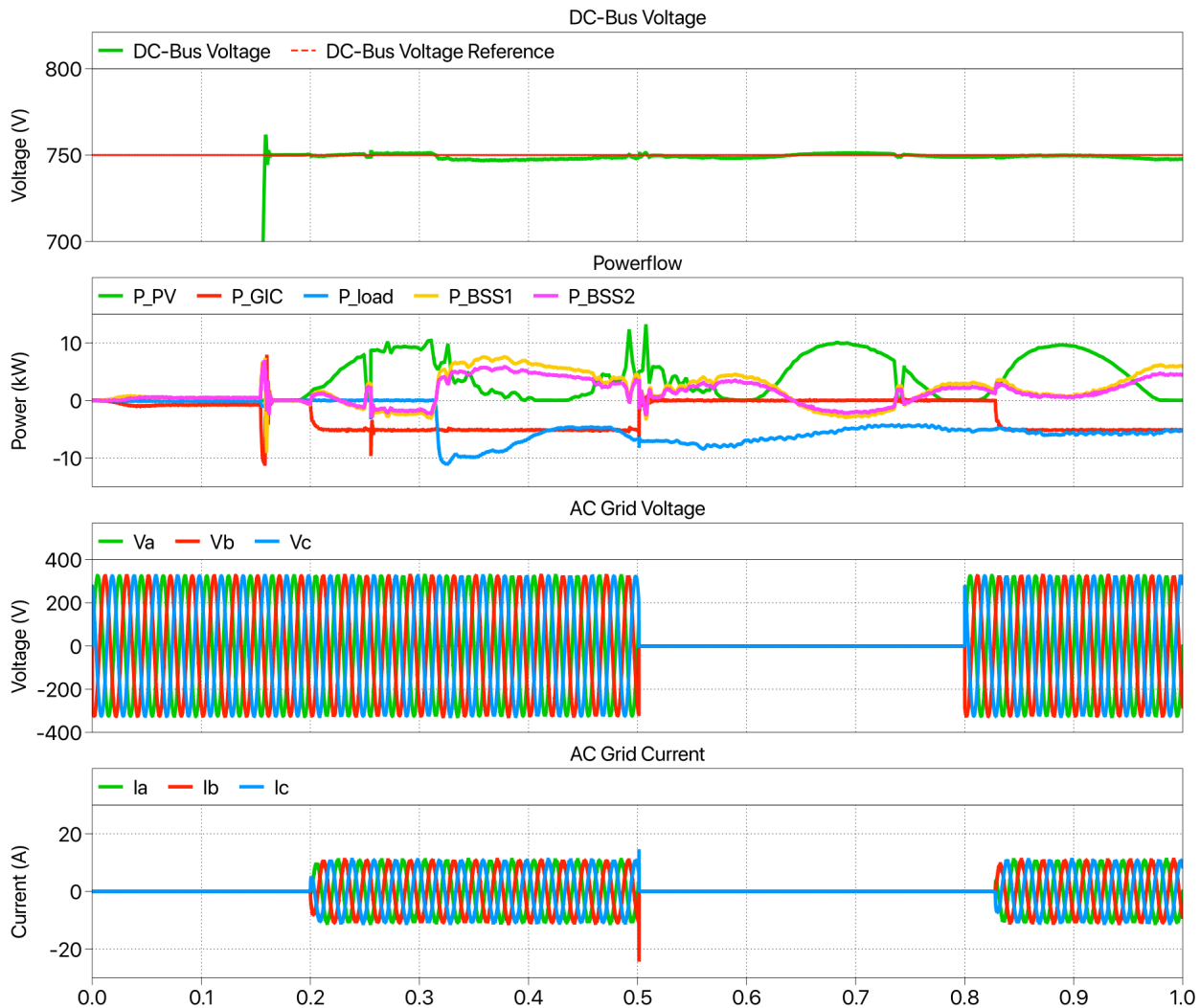


Figure 12: The figure caption of the simulation results

4 Conclusion

This model demonstrates the simulation of an entire DC microgrid that supports embedded code generation for TI C2000 MCUs. The hardware of the test system comprises 4 RT Boxes to simulate the different physical parts of the overall power system and 3 TI Launchpads to implement the local control units of the converters. The whole offline and real-time deployment can be done from one single PLECS model as well as the monitoring of simulation results and real-time operation. Further development on this comprehensive microgrid model may include additional power loads and sources as well as a supervisory/centralized controller that communicates to the local control units of each converter.

References

- [1] GAO, F., KANG, R., CAO, J. et al., *Primary and secondary control in DC microgrids: a review.*, J. Mod. Power Syst. Clean Energy 7, 2019, 227-242. [Online]. Available:

<https://link.springer.com/article/10.1007/s40565-018-0466-5>.

- [2] TI C2000 Piccolo MCU F28069M LaunchPad development kit,
URL: <http://www.ti.com/tool/LAUNCHXL-F28069M>.
- [3] TI C2000 Delfino MCU F28379D LaunchPad development kit,
URL: <http://www.ti.com/tool/LAUNCHXL-F28379D>.

Revision History:

C2000 TSP 1.1.1	First release
C2000 TSP 1.4.5	Updated the powerstage protection parameters, and web links
C2000 TSP 1.5.1	Minimized the usage of double-precision math in the controller, and set the Sync to "Self" on PWM2
C2000 TSP 1.6.1	Added auto-pin selection

How to Contact Plexim:

☎	+41 44 533 51 00	Phone
	+41 44 533 51 01	Fax
✉	Plexim GmbH Technoparkstrasse 1 8005 Zurich Switzerland	Mail
@	info@plexim.com	Email
	http://www.plexim.com	Web

Embedded Code Generation Demo Model

© 2002–2023 by Plexim GmbH

The software PLECS described in this document is furnished under a license agreement. The software may be used or copied only under the terms of the license agreement. No part of this manual may be photocopied or reproduced in any form without prior written consent from Plexim GmbH.

PLECS is a registered trademark of Plexim GmbH. MATLAB, Simulink and Simulink Coder are registered trademarks of The MathWorks, Inc. Other product or brand names are trademarks or registered trademarks of their respective holders.